

Intense cross-tail field-aligned currents in the plasma sheet at lunar distances

Sixue Xu^{1,2}, Andrei Runov¹, Anton Artemyev^{1,3}, Vassilis Angelopoulos¹, and Quanming Lu²

Field-aligned currents in the Earth's magnetotail are traditionally associated with transient plasma flows and strong plasma pressure gradients in the near-Earth side. In this paper we demonstrate a new field-aligned current system present at the lunar orbit tail. Using magnetotail current sheet observations by two ARTEMIS probes at $\sim 60R_E$, we analyze statistically the current sheet structure and current density distribution closest to the neutral sheet. For about half of our 130 current sheet crossings, the equatorial magnetic field component across-the tail (along the main, cross-tail current) contributes significantly to the vertical pressure balance. This magnetic field component peaks at the equator, near the cross-tail current maximum. For those cases, a significant part of the tail current, having an intensity in the range $1\text{--}10\text{ nA/m}^2$, flows along the magnetic field lines (it is both field-aligned and cross-tail). We suggest that this current system develops in order to compensate the thermal pressure by particles that on its own is insufficient to fend off the lobe magnetic pressure.

Main point #1: Statistics of the magnetotail current sheet properties at the lunar orbit

Main point #2: Significant contribution of the magnetic field shear to the pressure balance for $\sim 50\%$ observed current sheets

Main point #3: Intense field-aligned currents ($1 - 10\text{ nA/m}^2$) at the lunar orbit magnetotails.

1. Introduction

Dynamics large-scale plasma systems, planetary magnetotails, is significantly determined by configuration of the magnetotail current sheets, regions with strong plasma currents [e.g., Eastwood *et al.*, 2015, and references therein]. The Earth magnetotail current sheet, most accessible for in-situ spacecraft investigations, represents the high- β region where the plasma pressure significantly exceeds the magnetic field pressure. Models describing the such configuration predicts strong cross-tail currents (from dawn to dusk) flowing across the magnetic field [see, e.g., Birn *et al.*, 2004; Zelenyi *et al.*, 2011; Sitnov and Merkin, 2016, and references

therein]. This concept is based on an assumption of the diamagnetic nature of magnetotail currents. Strong deviations from this nominal geometry and formations of cross-tail currents flowing locally along magnetic field lines were observed in the near-Earth plasma sheet during flapping events [e.g., Petrukovich *et al.*, 2008] and during current sheet thinning [Artemyev *et al.*, 2016]. Yet, the geometry of currents in the mid-distant magnetotail remains unknown.

At the lunar orbit the Earth dipole magnetic field is vanishing and the average positive north-south component B_z (GSM coordinates are used through the paper) is smaller than B_z fluctuations. The lack of the dipole-dominated magnetic field configuration [the lunar orbit magnetotail is more influenced by solar wind conditions than by Earth dipole field, see, e.g., Sibeck and Lin, 2014, and references therein] and the presence of transient intense currents [e.g., Pulkkinen *et al.*, 1993; Vasko *et al.*, 2015] make the magnetotail current sheet very dynamical and unstable. Therefore, one can expect an existing of more complicated and exotic current sheet configuration in the mid-distant tail in comparison with the near-Earth controlled by the Earth dipole field. An important question is how global magnetotail dynamics (e.g., rotation of the equatorial plane following the interplanetary magnetic field, large-scale flapping waves, etc.) deform the current sheet and can these deformations result in new current sheet configuration including field-aligned currents?

To address this question, we investigate the current sheet properties at the lunar orbit ($\sim -60R_E$) using two ARTEMIS (Acceleration, Reconnection, Turbulence, and Electrodynamics of the Moon's Interaction with the Sun) probes. Being interested in local current sheet structure, we focus on flapping current sheets and use plasma velocity to reconstruct the spatial scales and current densities [Sergeev *et al.*, 1998]. Collected statistics of the current sheet observations reveal previously unknown property of this magnetotail region: about half of observed sheets are characterised by significant contribution of the magnetic field shear to the pressure balance. Such atypical for the Earth magnetotail current sheets have a local equatorial peak of the magnetic field component directed along the current density and the corresponding intense cross-tail field-aligned currents with magnitudes $\sim 1 - 10\text{ nA/m}^2$. Similar current sheet configurations are frequently observed in solar wind [e.g., Paschmann *et al.*, 2013] and planetary magnetotails where plasma pressure can be insufficiently high to support the pressure balance [e.g., Jupiter, Venus, Mars, see Artemyev *et al.*, 2014; Rong *et al.*, 2015; Artemyev *et al.*, 2017], but in the near-Earth magnetotail such current sheet configuration were found only within close vicinity of the reconnection region [e.g., Nakamura *et al.*, 2008]. In contrast, we have demonstrate that at the lunar orbit the current sheets with intense cross-field field-aligned currents are very representative state of the magnetotail current sheet.

2. Data Set and Analysis Technique

Since July 2011 both ARTEMIS probes (P1 and P2) has been in stable equatorial, high-eccentricity, 26-hr period orbits $\sim 100\text{ km} \times 19,000\text{ km}$ altitude over the Moon. The inter-probe separations varies between 500 km and $5R_E$. The

¹Institute of Geophysics and Planetary Physics, University of California, Los Angeles, USA

²CAS Key Laboratory of Geospace Environment, Department of Geophysics and Planetary Sciences, University of Science and Technology of China, Hefei, China

³Space Research Institute, RAS, Moscow, Russia

ARTEMIS duo traverses the magnetotail during about four days per a month. In this study we use measurements of the ARTEMIS fluxgate magnetometer [16 vectors per second in fast survey, see *Auster et al.*, 2008] and ion moments provided by combined data of the electrostatic analyzer [ESA, energies below ~ 25 keV energies *McFadden et al.*, 2008] and solar state telescope [*Angelopoulos et al.*, 2008]. For electron moment we use only ESA measurements. We use only fast survey data, what determines the dominance of observations in the duskside ($Y_{GSM} > 0$).

For one year of ARTEMIS observation (from June 2016 to June 2017) we visually select all current sheet crossings (130 events) characterized by B_x reversal within less than 20 min and with the B_x span larger than 5 nT. To determine the local coordinate system, we use the minimum variance analysis (MVA) resulting in the \mathbf{l} , \mathbf{m} , and \mathbf{n} vectors of maximum, medium, and minimum variances, respectively [*Sonnerup and Cahill*, 1968]. The maximum variance direction is mainly along the sign-changes component (B_x), the minimum variance direction is treated as the normal to a plane current sheet (i.e., direction of the main gradient), and the intermediate variance direction is along the nominal electric current direction.

We have checked that for all selected currents sheets the pressure balance $B_l^2 + B_m^2 + 2k_B\mu_0 n_e(T_i + T_e) = B_{lobe}^2 \approx \text{const}$ is satisfied within 20% (here n_e , T_i , T_e are electron density, ion and electron temperatures). The pressure balance analysis reveals two distinct categories of current sheet structure: 1) currents sheets where the magnetic pressure $B_{lobe}^2 \gg B_m^2$ is fully balanced by the thermal plasma pressure $2k_B\mu_0 n_e(T_e + T_i)$, and 2) current sheets with large contribution of B_m variation to the pressure balance. In the latter cases, B_m^2 peaks around the equatorial plane $B_l = 0$ and the B_m^2 variation across the sheet ΔB_m^2 comparable to $\Delta B_l^2 \approx B_{lobe}^2$. Figure 1(a) shows spatial (in (X, Y) GSM aberrated on 4°) distribution of current sheets with $\Delta B_m^2/B_{lobe}^2 < 0.2$ and $\Delta B_m^2/B_{lobe}^2 > 0.2$ (with $B_m \gtrsim 0.4B_{lobe}$). A significant population of selected current sheets are characterized by B_m contribution to the pressure balance. This is distinctive feature of the middle (lunar orbit) magnetotail, whereas in the near-Earth tail the current sheets with $B_m \gtrsim 0.4B_{lobe}$ are observed quite rare [see few examples in *Nakamura et al.*, 2008; *Rong et al.*, 2012].

Figure 1(b) illustrated the correlation between electron number density (blue point), normalized thermal pressure ($2k_B\mu_0 n_e(p_i + p_e)/B_{lobe}^2$, red cross) and $\Delta B_m^2/B_{lobe}^2$. Most of events are concentrated in the lower diagonal side, i.e. current sheets with large $\Delta B_m^2/B_{lobe}^2$ are characterized by low density (low plasma pressure), whereas current sheets with large density (thermal pressure) are characterised by small $\Delta B_m^2/B_{lobe}^2$. As showed in Fig. 1(c), among the 130 events, half of them fall in to the first category with insignificant B_m contribution to the pressure balance, and the

other half have large ΔB_m showing a long-tail distribution of $\Delta B_m^2/B_{lobe}^2$ ranging from 0.2 to 1.0.

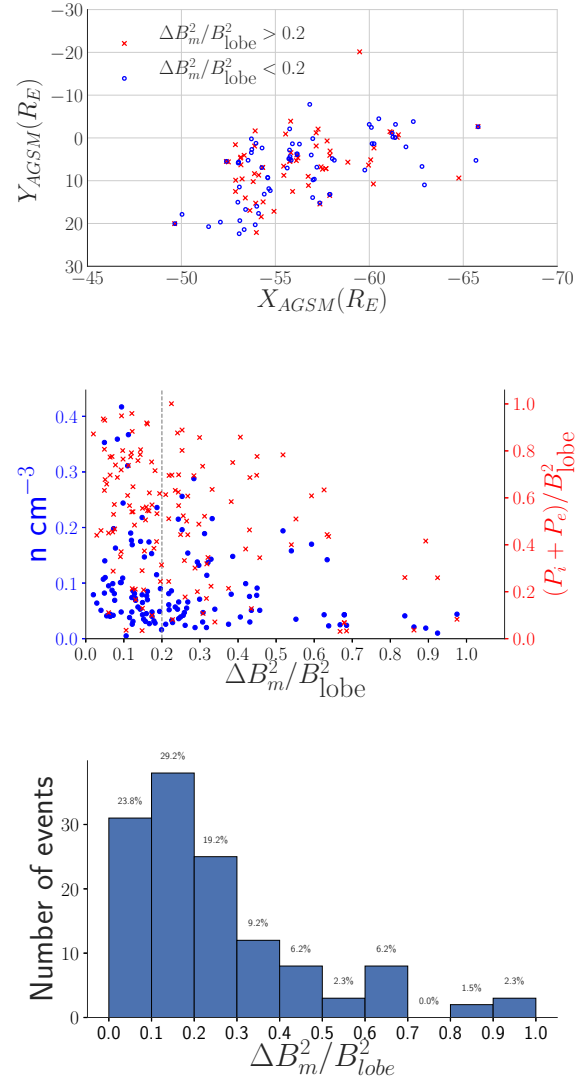


Figure 1. (a) distribution of current sheets with $\Delta B_m^2/B_{lobe}^2 < 0.2$ (blue circles) and $\Delta B_m^2/B_{lobe}^2 > 0.2$ (red crosses). (b) plasma density and thermal pressure in the current sheet center $|B_l| < 0.4B_{lobe}$ nT as functions of $\Delta B_m^2/B_{lobe}^2$. (c) histogram of $\Delta B_m^2/B_{lobe}^2$ distribution.

3. Current sheet internal structure

To investigate the inner structure of the current sheets with large $\Delta B_m^2/B_{lobe}^2$, we select five cases with the v_z (or $\mathbf{v} \cdot \mathbf{n}$) velocity well correlating with dB_l/dt that enable us to use the reconstruction technique [*Sergeev et al.*, 1998]. Table 1 shows main parameters of these current sheets (events A-E). For all events, except A, the ratio of eigenvalues of \mathbf{m} and \mathbf{n} vectors are large enough to distinguish well between \mathbf{m} and \mathbf{n} directions. Interplanetary magnetic field B_y (IMF) measured within 30 minutes including the time interval of the current sheet observations is relatively small (≤ 1 nT).

Table 1. characteristic parameters of selected crossings

Case	date	time	λ_m/λ_n	$\Delta B_m^2/B_{\text{lobe}}^2$	IMF B_y nT	B_{lobe} nT	N_i cm $^{-3}$	$p_e + p_i$ nT 2	j_l nA/m 2	j_m nA/m 2	L km	L/ρ_i
A	2017-04-13	01:02:38	2.149	0.253	-1.27	7.30	0.20	47.36	0.45	1.25	4895	11.05
B	2017-01-11	18:37:00	15.000	0.552	-0.97	8.78	0.04	39.28	-9.06	-12.16	492	0.76
C	2017-01-11	11:40:33	7.042	0.593	-0.45	8.76	0.17	46.70	2.50	-2.05	1721	3.90
D	2016-11-13	19:48:18	16.601	0.317	0.76	11.85	0.02	24.06	8.06	-13.53	516	1.17
E	2016-10-15	08:08:06	6.322	0.634	-6.68	14.46	0.14	92.75	-11.09	8.90	689	1.91
F	2017-01-11	10:45:16	1.864	0.02	0.60	9.66	0.08	81.37	0.10	-0.69	5404	8.07

Using the linear regression between dB_l/dt and v_z , we estimate the current densities $j_m \sim (dB_l/dt)/v_z$, $j_l \sim (dB_m/dt)/v_z$ and current sheet spatial scale (thickness, L). Table 1 shows that j_m can reach 10 nA/m^2 [quite large value even in comparison with the near-Earth current sheet, see review *Petrukovich et al.*, 2015]. Current sheet thicknesses are about $500 - 1000 \text{ km}$ and comparable with the ion gyroradius calculated in B_{lobe} . Thus, we deal with thin current sheets. The magnitude of j_l current is comparable with j_m magnitude, what makes selected current sheets different from the typical magnetotail current sheets with $j_l \sim 0$. For a comparison, we also select one example of flapping current sheet with well correlated v_n and dB_l/dt , but without significant ΔB_m^2 (event F from Table 1).

Figure 2 shows three sets of six panels with current sheet characteristics. The top panels demonstrate time series of magnetic field components (gray curves show well established pressure balance, $B_{\text{lobe}} \approx \text{const}$). There is clear B_m peak around the equatorial plane $B_l = 0$ for events A-E. In all cases, n_y component is significant, i.e. we deal with tilted current sheets [*Zhang et al.*, 2002], where current density flow partially along the north-south direction, whereas B_m component is contributed both by GSM B_y and B_z . Although, the near-Earth observations revealed strong field-aligned currents in the tilted current sheets [e.g., *Petrukovich et al.*, 2015, and references therein], these currents were generated due to $j_m \sim j_z$ projection to uniform $B_m \sim B_z$ field, whereas strong peak of $B_m \sim B_z, B_y$ has not been reported yet.

Middle panels of Fig. 2 show profiles of plasma and ΔB_m^2 pressures versus B_l . For five selected current sheets the B_m contribution to the pressure balance is comparable with the thermal plasma contribution. Variation of the plasma pressure across the current sheets is supported both by density and temperature variations (see bottom panels of Fig. 2). Density distributions of Case A, C, E show a decrease of $\sim 50\%$, $\sim 30\%$, $\sim 25\%$ from the maximum value at $B_l = 0$.

In Case A, C, F, the temperature has almost uniform profile across the sheet, whereas in Case B, D, E, the temperature decreases to 50% of its maximum value at $B_l = 0$. The temperature increase in case C at the current sheet boundary is due to very rarefied hot field-aligned ion flows. It is interesting to note strong density variations across the sheet in cases A, E and F. In the near-Earth magnetotail, temperature variations across the sheet, $T_i(B_l)$, are usually stronger than the density variation [e.g., *Runov et al.*, 2006; *Petrukovich et al.*, 2015].

To reconstruct the internal current sheet structure, we adopt methods used by *Sergeev et al.* [1998], *Vasko et al.* [2015] and determine time interval with good correlation between derivative dB_l/dt of the 16s smoothed magnetic field and v_n (or v_z) velocity. Then we integrate velocity (excluding offset v_0 defined from $dB_l/dt = \mu_0 j_m v_z + v_0$ fitting) along this interval to determine z coordinate ($z = 0$ is defined at $B_l = 0$). We fit $B_l(z)$ and $B_m(z)$ dependencies by simple function $\tanh(z/L)$, $\cosh^{-1}(z/L)$ [see model in *Harrison and Neukirch*, 2009]. Top six panels of Fig. 3 shows these magnetic field profiles. For events A-E the B_m component demonstrates the clear bell-shaped profile, $B_m \sim \cosh^{-1}(z/L)$, with the current sheet thickness L about few ion gyroradii.

Using fitted magnetic fields, we estimate the current density profiles. Bottom six panels in Fig. 3 shows strong peak of $j_m \sim 1 - 10 \text{ nA/m}^2$ and bi-polar j_l profiles for events A-E. The event F is characterized by rather weak $j_m \sim 0.5 \text{ nA/m}^2$ [this is typical current density magnitude at such distances, see *Vasko et al.*, 2015]. The large B_m makes from almost all measured cross-tail j_m the field-aligned current. The transverse current magnitude usually several times smaller than the field-aligned current. Interesting, due to different B_m direction and different normal \mathbf{n} direction, the measured field-aligned current can be positive or negative (from event to event).

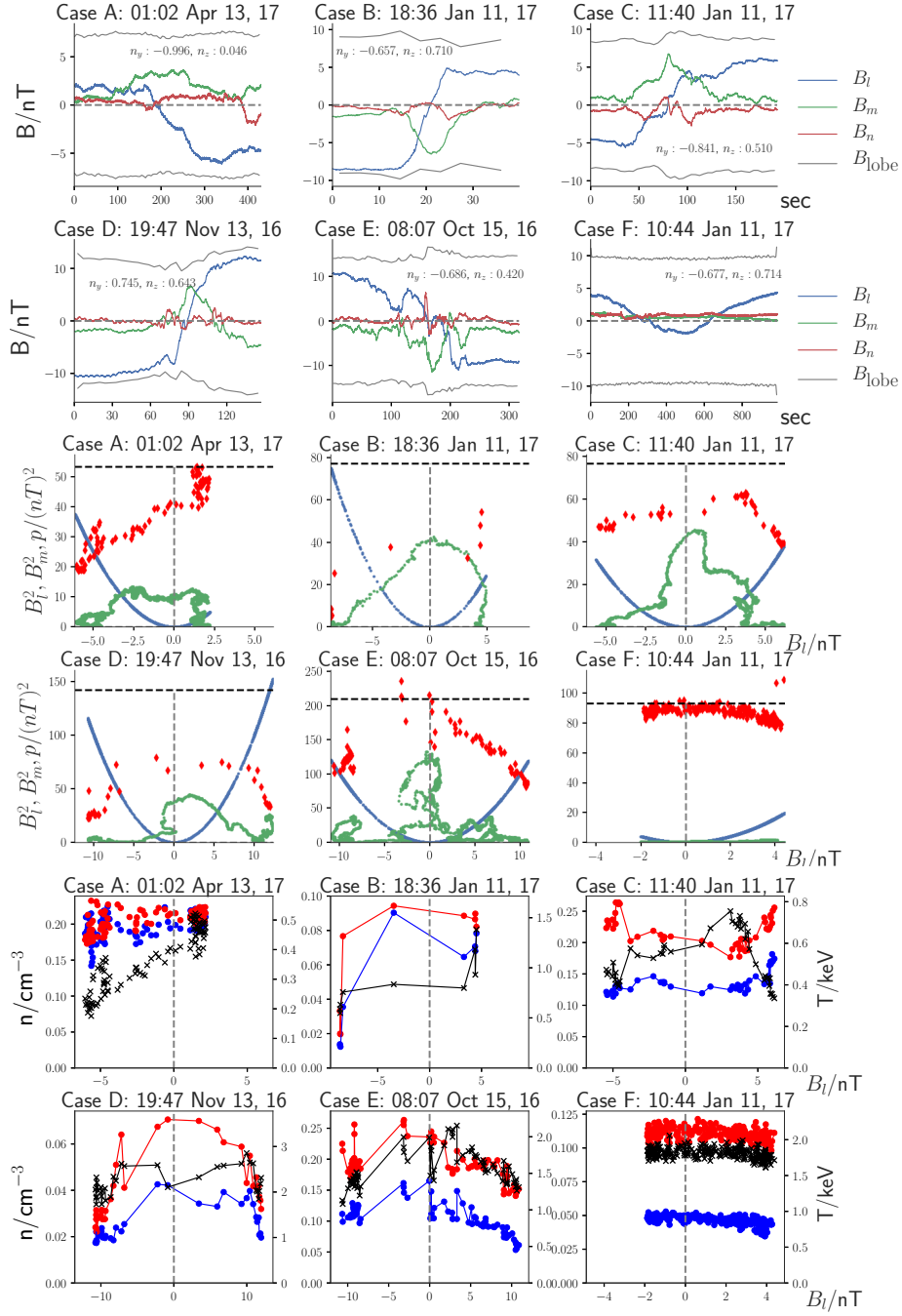


Figure 2. Top six panels show time series of magnetic field components and lobe magnetic field (grey curve). Middle six panels show pressure components B_l^2 (blue), B_m^2 (green), and $p = 2\mu_0 k_B n_e (T_i + T_e)$ (red), the top dashed lines indicate the average lobe pressure. Bottom six panels show distributions of the density (black cross) and ion (red), electron (blue) temperatures across the sheet. The electron temperature is multiplied by 5.

4. Discussion and Conclusions

We have demonstrated that a significant population of current sheets observed by ARTEMIS at the lunar orbit consists of atypical current sheet configurations with strong B_m peak around the equatorial plane $B_l = 0$. These current sheets are tilted with the normal partially directed along dawn-dusk. The B_m peak is provided both by GSM B_z and B_y increase and contribute significantly to the pressure balance. Existing of such specific current sheets can be related to low plasma pressure (low density, temperature) which is insufficient to balance the lobe (solar wind) pressure $\sim B_{\text{lobe}}^2$. Similar current sheet configurations were found in rarefied plasma of the Jupiters magnetotail [Artemyev et al., 2014] and in cold plasma of Mars and Venus magnetotails [Rong et al., 2015; Artemyev et al., 2017]. In the Jupiter magnetotail current sheets controlled by strong planet magnetic field, and observed field-aligned currents represent the part of the global magnetosphere current system. Instead, Mars and Venus magnetotails form mainly by the solar wind magnetic field (due to absence of regular planetary magnetic field) and currents sheets in these magnetospheres resemble the solar wind rotational discontinuities [e.g., Paschmann et al., 2013, and references therein]. The Earth magnetotail probed by ARTEMIS spacecraft represents some intermediate state between Jupiter magnetotail filled by rarefied plasma but strongly connected to planetary magnetic field and Mars/Venus magnetotail filled by cold plasma and IMF field lines. A closure of the intense field-aligned currents observed at lunar orbit is unknown and needs to be investigated with global models. Independently on the current closure, the observation of the statistically significant population of that atypical current sheets at lunar orbit opens a challenge for simulations and theories of the current sheet configuration.

Significant change in the current sheet configuration (in comparison with a simple diamagnetic configuration of the near-Earth tail) should result in change of the stability conditions and dynamical properties. In-

deed, numerical simulations shows distinguishing features in magnetic reconnection initialization and development in current sheets with strong cross-tail field-aligned currents [e.g., Zhou et al., 2015; Wilson et al., 2016; Fan et al., 2016]. The primary region of the magnetotail reconnection ($\sim 30 - 40 R_E$) is located right between the well investigated near-Earth current sheet with strong transverse cross-tail currents [see statistics of Cluster results in Runov et al., 2006; Petrukovich et al., 2015] and the lunar distant current sheet with strong cross-tail field-aligned currents. Therefore, current sheets at $\sim 30 - 40 R_E$ can share properties of both these current sheet population and destabilization of this sheets can involve intensification of both transverse and field-aligned currents. This problem can be addressed by Magnetospheric Multiscale mission operating exactly within this region [Burch et al., 2016] and having chance to investigate the internal structure cross-tail field-aligned currents

Acknowledgments. We acknowledge NASA contract NAS502099 for the use of data from the THEMIS Mission. We would like to thank the following people specifically C. W. Carlson and J. P. McFadden for the use of ESA data, D.E. Larson and R.P. Lin for the use of SST data, and K.H. Glassmeier, U. Auster, and W. Baumjohann for the use of FGM data provided under the lead of the Technical University of Braunschweig and with financial support through the German Ministry for Economy and Technology and the German Aerospace Center (DLR) under contract 50 OC 0302.

The THEMIS data were downloaded from <http://themis.ssl.berkeley.edu/>.

References

- Angelopoulos, V., et al., First Results from the THEMIS Mission, *Space Sci. Rev.*, *141*, 453–476, doi:10.1007/s11214-008-9378-4, 2008.
- Artemyev, A. V., I. Y. Vasko, and S. Kasahara, Thin current sheets in the Jovian magnetotail, *Planetary Space Science*, *96*, 133145, doi:10.1016/j.pss.2014.03.012, 2014.
- Artemyev, A. V., V. Angelopoulos, J. Liu, and A. Runov, Electron currents supporting the near-earth magnetotail during current sheet thinning, *Geophys. Res. Lett.*, , pp. n/a–n/a, doi:10.1002/2016GL072011, 2016.
- Artemyev, A. V., V. Angelopoulos, J. S. Halekas, A. Runov, L. M. Zelenyi, and J. P. McFadden, Mars's magnetotail: Nature's current sheet laboratory, *J. Geophys. Res.*, *122*, 5404–5417, doi:10.1002/2017JA024078, 2017.
- Auster, H. U., et al., The THEMIS Fluxgate Magnetometer, *Space Sci. Rev.*, *141*, 235–264, doi:10.1007/s11214-008-9365-9, 2008.

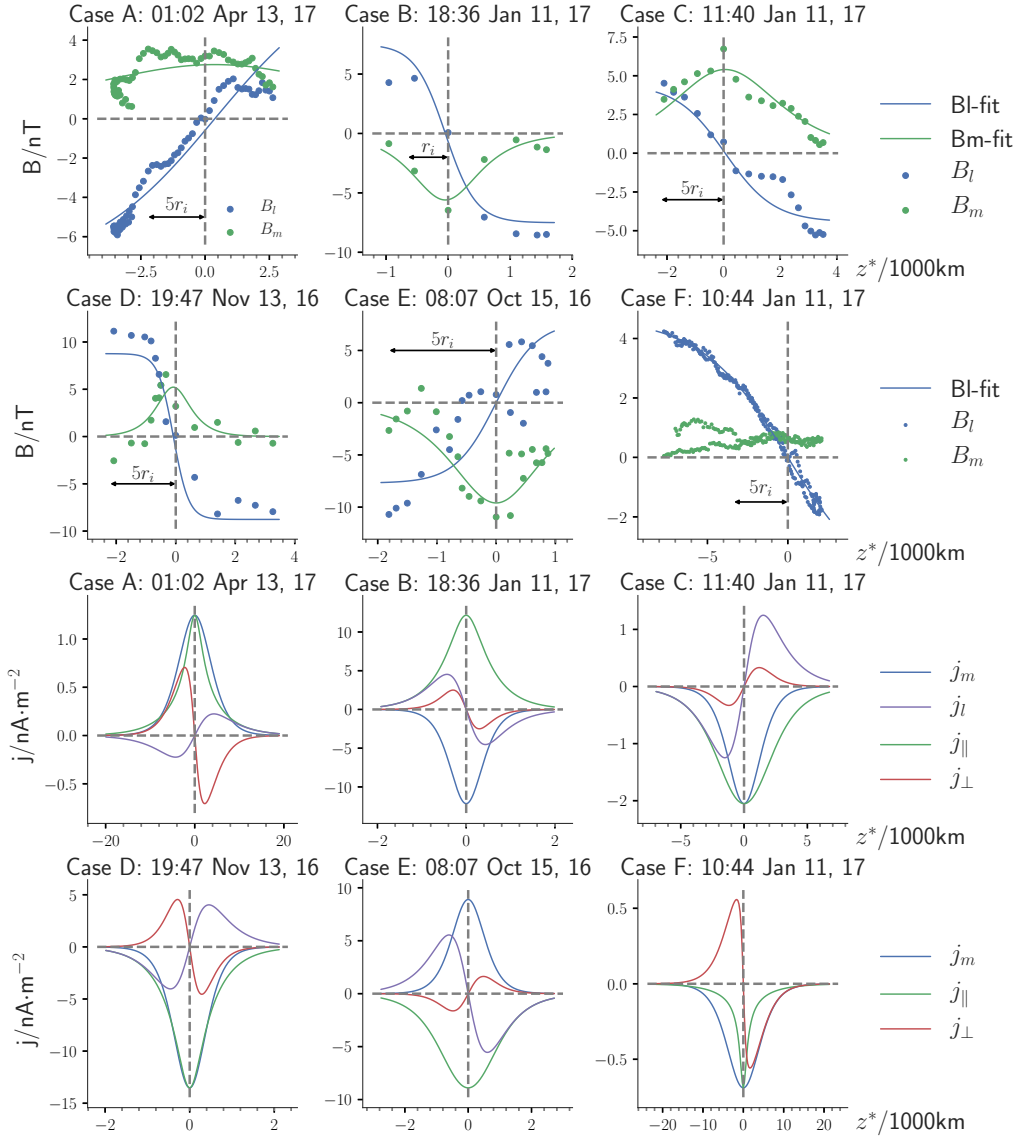


Figure 3. Top six panel shows the reconstructed spatial profile of B_l, B_m , whereas bottom six panels show $j_l, j_m, j_{||}, j_{\perp}$ profiles.

- Birn, J., K. Schindler, and M. Hesse, Thin electron current sheets and their relation to auroral potentials, *J. Geophys. Res.*, **109**, 2217, doi:10.1029/2003JA010303, 2004.
- Burch, J. L., T. E. Moore, R. B. Torbert, and B. L. Giles, Magnetospheric Multiscale Overview and Science Objectives, *Space Sci. Rev.*, **199**, 5–21, doi:10.1007/s11214-015-0164-9, 2016.
- Eastwood, J. P., H. Hietala, G. Toth, T. D. Phan, and M. Fujimoto, What Controls the Structure and Dynamics of Earth's Magnetosphere?, *Space Sci. Rev.*, **188**, 251–286, doi: 10.1007/s11214-014-0050-x, 2015.
- Fan, F., C. Huang, Q. Lu, J. Xie, and S. Wang, The structures of magnetic islands formed during collisionless magnetic reconnections in a force-free current sheet, *Physics of Plasmas*, **23**(11), 112106, doi:10.1063/1.4967286, 2016.
- Harrison, M. G., and T. Neukirch, One-Dimensional Vlasov-Maxwell Equilibrium for the Force-Free Harris Sheet, *Physical Review Letters*, **102**(13), 135,003, doi: 10.1103/PhysRevLett.102.135003, 2009.
- McFadden, J. P., C. W. Carlson, D. Larson, M. Ludlam, R. Abiad, B. Elliott, P. Turin, M. Marckwordt, and V. Angelopoulos, The THEMIS ESA Plasma Instrument and In-flight Calibration, *Space Sci. Rev.*, **141**, 277–302, doi: 10.1007/s11214-008-9440-2, 2008.
- Nakamura, R., et al., Cluster observations of an ion-scale current sheet in the magnetotail under the presence of a guide field, *J. Geophys. Res.*, **113**, A07S16, doi:10.1029/2007JA012760, 2008.
- Paschmann, G., S. Haaland, B. Sonnerup, and T. Knetter, Discontinuities and Alfvénic fluctuations in the solar wind, *Annales Geophysicae*, **31**, 871–887, doi:10.5194/angeo-31-871-2013, 2013.
- Petrkovich, A. A., W. Baumjohann, R. Nakamura, and A. Runov, Formation of current density profile in tilted current sheets, *Annales Geophysicae*, **26**, 3669–3676, 2008.

- Petrukovich, A. A., A. V. Artemyev, I. Y. Vasko, R. Nakamura, and L. M. Zelenyi, Current sheets in the Earth magnetotail: plasma and magnetic field structure with Cluster project observations, *Space Sci. Rev.*, *188*, 311337, doi:10.1007/s11214-014-0126-7, 2015.
- Pulkkinen, T. I., D. N. Baker, C. J. Owen, J. T. Gosling, and N. Murphy, Thin current sheets in the deep geomagnetic tail, *Geophys. Res. Lett.*, *20*, 2427–2430, doi:10.1029/93GL01590, 1993.
- Rong, Z. J., et al., Profile of strong magnetic field B_y component in magnetotail current sheets, *J. Geophys. Res.*, *117*, A06216, doi:10.1029/2011JA017402, 2012.
- Rong, Z. J., et al., The flapping motion of the Venusian magnetotail: Venus Express observations, *J. Geophys. Res.*, *120*, 5593–5602, doi:10.1002/2015JA021317, 2015.
- Runov, A., et al., Local structure of the magnetotail current sheet: 2001 Cluster observations, *Annales Geophysicae*, *24*, 247–262, 2006.
- Sergeev, V., V. Angelopoulos, C. Carlson, and P. Sutcliffe, Current sheet measurements within a flapping plasma sheet, *J. Geophys. Res.*, *103*, 9177–9188, doi:10.1029/97JA02093, 1998.
- Sibeck, D. G., and R.-Q. Lin, Size and shape of the distant magnetotail, *J. Geophys. Res.*, *119*, 1028–1043, doi:10.1002/2013JA019471, 2014.
- Sitnov, M. I., and V. G. Merkin, Generalized magnetotail equilibria: Effects of the dipole field, thin current sheets, and magnetic flux accumulation, *J. Geophys. Res.*, *121*, 7664–7683, doi:10.1002/2016JA023001, 2016.
- Sonnerup, B. U. Ö., and L. J. Cahill, Jr., Explorer 12 observations of the magnetopause current layer, *J. Geophys. Res.*, *73*, 1757, doi:10.1029/JA073i005p01757, 1968.
- Vasko, I. Y., A. A. Petrukovich, A. V. Artemyev, R. Nakamura, and L. M. Zelenyi, Earth's distant magnetotail current sheet near and beyond lunar orbit, *J. Geophys. Res.*, *120*, 8663–8680, doi:10.1002/2015JA021633, 2015.
- Wilson, F., T. Neukirch, M. Hesse, M. G. Harrison, and C. R. Stark, Particle-in-cell simulations of collisionless magnetic reconnection with a non-uniform guide field, *Physics of Plasmas*, *23*(3), 032302, doi:10.1063/1.4942939, 2016.
- Zelenyi, L. M., H. V. Malova, A. V. Artemyev, V. Y. Popov, and A. A. Petrukovich, Thin current sheets in collisionless plasma: Equilibrium structure, plasma instabilities, and particle acceleration, *Plasma Physics Reports*, *37*, 118–160, doi:10.1134/S1063780X1102005X, 2011.
- Zhang, T. L., W. Baumjohann, R. Nakamura, A. Balogh, and K. Glassmeier, A wavy twisted neutral sheet observed by CLUSTER, *Geophys. Res. Lett.*, *29*(19), 190,000, doi:10.1029/2002GL015544, 2002.
- Zhou, F., C. Huang, Q. Lu, J. Xie, and S. Wang, The evolution of the ion diffusion region during collisionless magnetic reconnection in a force-free current sheet, *Physics of Plasmas*, *22*(9), 092110, doi:10.1063/1.4930217, 2015.

Sixue Xu, Department of Geophysics and Planetary Science, University of Science and Technology of China, Hefei, China (hxxsx@mail.ustc.edu.cn)

Andrei Runov, Institute of Geophysics and Planetary Physics, University of California, Los Angeles, USA

Anton Artemyev, Institute of Geophysics and Planetary Physics, University of California, Los Angeles, USA

Vassilis Angelopoulos, Institute of Geophysics and Planetary Physics, University of California, Los Angeles, USA

Quanming Lu, CAS Key Laboratory of Geospace Environment, Department of Geophysics and Planetary Science, University of Science and Technology of China, Hefei, China (qmlu@ustc.edu.cn)